

MODEL ATMOSPHERES AND QUANTITATIVE SPECTROSCOPY OF LUMINOUS BLUE STARS

R.P. KUDRITZKI, A. GABLER,
R. GABLER, H.G. GROTH,
A.W.A. PAULDRACH, J. PULS
Universitäts-Sternwarte München

ABSTRACT. The basic physics of model atmospheres for Luminous Blue Stars (LBS) are discussed. The discussion comprises the model description of both subsonic photospheres and supersonic winds and the application of model calculations for the purpose of quantitative spectroscopy.

1. THE BASIC PHYSICS OF PHOTOSPHERES

1.1. The definition of "photospheres" and "winds"

Since the term "photosphere" has been used several times during this meeting with a different meaning, we want to give our definition at the beginning of this paper. Photospheres are the subsonic layers (wind outflow velocity $v(r) \ll v_{\text{sound}}$), which in the case of OB-stars normally emit the optical and UV continuum, the weak lines and the wings of the hydrogen and helium lines. The layers of supersonic outflow we call "winds".

In extreme cases - such as LBVs in outburst - it might occur that photospheres do not exist and that the whole continuum is also formed in the wind. However, in all normal situations of OB-stars including the quiescent phase of LBVs this definition is very useful. It allows us to approximate the density structure of the photospheres of LBS by a simple hydrostatic description which is sufficiently accurate (see Kudritzki, 1988, hereafter Ku 88). In the following we discuss the basic physics of these photospheres.

1.2. Departures from LTE

LBS have an intense radiation field and rather low photospheric density. This means that collisions between electrons and ions are rare compared with radiative transitions. As a consequence NLTE effects dominate throughout the entire atmosphere. Although this has been well known for almost 20 years, it is worthwhile to give a significant exam-

ple. Fig. 1 shows the H_I line profile in LTE and NLTE calculated for $T_{\text{eff}} = 45000 \text{ K}$ and $\log g = 3.6$, parameters typical for an O4f-star. Similar striking differences are found for the HeI and HeII lines. It is thus obvious that LTE completely fails to describe the observed spectra (for a recent discussion, see Ku 88).

Since NLTE effects are expected to become smaller towards higher $\log g$ and lower T_{eff} , it is important to investigate where they become negligible with respect to the model atmosphere structure. This is summarized in Fig. 2. The borderline in these figures is the curve where the difference between NLTE and LTE H_I equivalent width is equal to 15%. In the NLTE domain the differences are larger, whereas they become smaller in the LTE domain. We see that for stars with $M_{\text{ZAMS}} \geq 25 M_{\odot}$ a NLTE treatment of their photospheres is inevitable. We note, however, that even in the LTE domain, careful NLTE calculations for complex metal ions are needed if one intends to determine accurate abundances from the metal lines (for examples see Ku 88).

1.3. Helium abundance

Almost as important as NLTE effects is the influence of the helium abundance. In particular, for LBS close to the Eddington-limit the observable quantities crucial for diagnostics like hydrogen lines, Balmer jump, (u-b) or (U-B) depend strongly on the helium abundance (see Kudritzki, 1973). In Fig. 3 we show a typical example for the case of A0 Ia supergiants ($T_{\text{eff}} = 10^4 \text{ K}$, $\log g = 1$): Hydrogen lines and Balmer jump become stronger with increasing helium abundance (i.e. decreasing hydrogen abundance)! Obviously a change from $N_{\text{He}}/N_{\text{H}} = 0.1$ to 1.0 is equivalent to an increase $\Delta \log g \approx 0.5$ for models with normal helium content. If we compare this apparent $\log g$ shift at $T_{\text{eff}} = 10^4 \text{ K}$ with the evolutionary tracks it is equivalent to a shift from the 60 M_{\odot} track down to 25 M_{\odot} or equivalent to $\Delta \log L/L \approx 0.8$. It is clear that this is of enormous relevance for the use of blue supergiants as distance indicators!

The reason for this effect is the influence of $N_{\text{He}}/N_{\text{H}}$ on effective gravity and density divided by opacity. A simple estimate for the pressure at optical depth unity yields (for details see Kudritzki, Groth, Humphreys, 1988, Astron. Astrophys., subm.):

$$P(\tau=1) \approx \frac{m_{\text{H}}}{\sigma_{\text{E}}} g (1 - \Gamma_{\text{O}} + 4 N_{\text{He}}/N_{\text{H}}),$$

$$\text{where } \Gamma_{\text{O}} = \frac{7.52}{g} \left(\frac{T_{\text{eff}}}{10^4} \right)^4 \quad (g \text{ in } \text{cm s}^{-2}, T_{\text{eff}} \text{ in K}).$$

Obviously, the helium abundance is as important as gravity for the atmospheric pressure structure for models close to the Eddington limit.

This effect might be the solution of a longstanding problem (Fehrenbach and Duflot, 1972, Humphreys, 1983, Dubois, 1986, Azzopardi, 1981). There exists a large group of B8 to A5 supergiants in the LMC as well as in the SMC with magnitudes that clearly point to luminosity class Ia. However, H_{γ} and H_{δ} are much too strong and U-B much too red (0.2 to 0.3 mag) and point to luminosity class II. This leads to a situation in which the B,A supergiants although brightest in M_V are obviously not useful as distance indicators. However, evolutionary tracks show that enhanced helium abundance in the photosphere of supergiants is to be expected (see also the following section), so that our effect can easily explain this observed discrepancy in principle. Of course, this has to be proven by detailed quantitative spectroscopy of A supergiants. Such a project is presently under way (Kudritzki, Groth, Humphreys). If successful, it will provide the means to use these optically brightest objects as distance indicators once more.

2. QUANTITATIVE SPECTROSCOPY OF LBS

2.1. Analysis method

The principle of the analysis is to use the profile fit of the hydrogen lines H_{γ} , H_{δ} for the determination of gravity and the profiles of HeI and HeII lines for the simultaneous determination of T_{eff} and helium abundance (for details see Ku 88 and references therein). Alternatively, for B-supergiants the use of other ionization equilibria (Si IV/III/II) or the energy distribution is necessary for T_{eff} , if the objects are too cool to show HeII lines. Note, however that here also $\log g$ has to be determined simultaneously, since the gravity influences the shape of the energy distribution significantly (Kudritzki et al., 1983, Fitzpatrick, 1987). Note also that the energy distribution method fails for O-stars (Hummer et al., 1988).

An important remark is necessary for all those objects, that have not yet been analysed quantitatively. Normally, an effective temperature is assigned in these cases according to their spectral type, which, following Conti and Alschuler (1971) and Conti and Frost (1977), is defined by $\log W' = \log W_{\lambda}(\text{HeI } 4471) - \log W_{\lambda}(\text{HeII } 4542)$. The dependency of $\log W'$ on both T_{eff} and $\log g$ is usually neglected. Fig. 4 shows that this simultaneous T_{eff} and $\log g$ dependence is important, in particular close to the Eddington-limit. This means that without a simultaneous gravity determination effective temperatures are extremely uncertain.

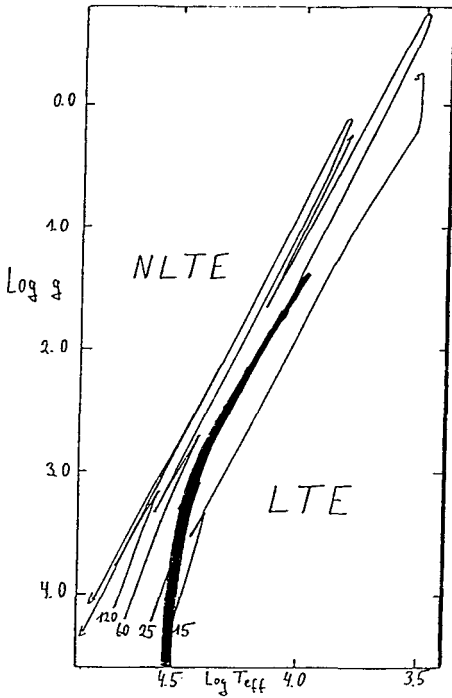


Fig. 2b: NLTE and LTE domain in the $(\log g, \log T_{\text{eff}})$ -plane.

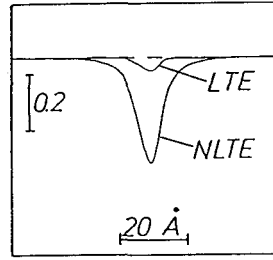


Fig. 1: Photospheric profile of H_{γ} calculated in LTE and NLTE for a typical O4f-star.

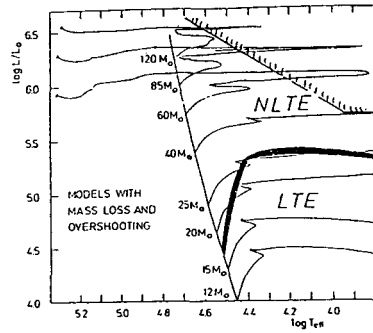


Fig. 2a: NLTE and LTE domain in the HR-diagram compared with tracks by MM (Maeder and Meynet, 1987).

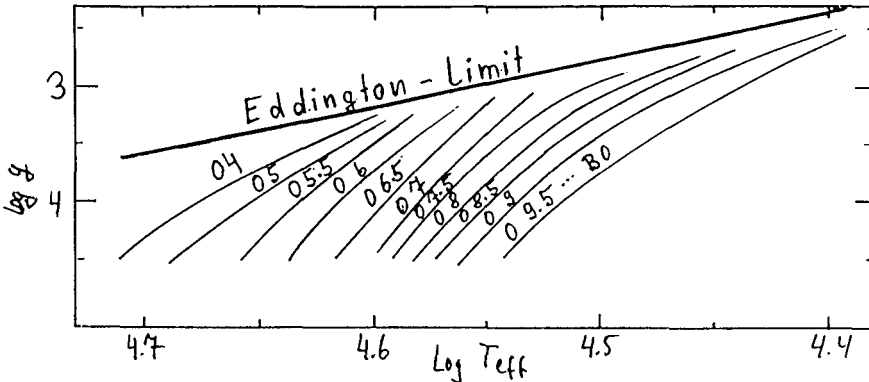


Fig. 4: The domain of the O-star spectral types in the $(\log g, \log T_{\text{eff}})$ -diagram. The spectral types are defined by the value of $\log W' = \log W_{\lambda}(\text{HeI } 4471) - \log W_{\lambda}(\text{HeII } 4542)$ (see Conti and Frost, 1977). Note that the spectral type depends on both T_{eff} and $\log g$.

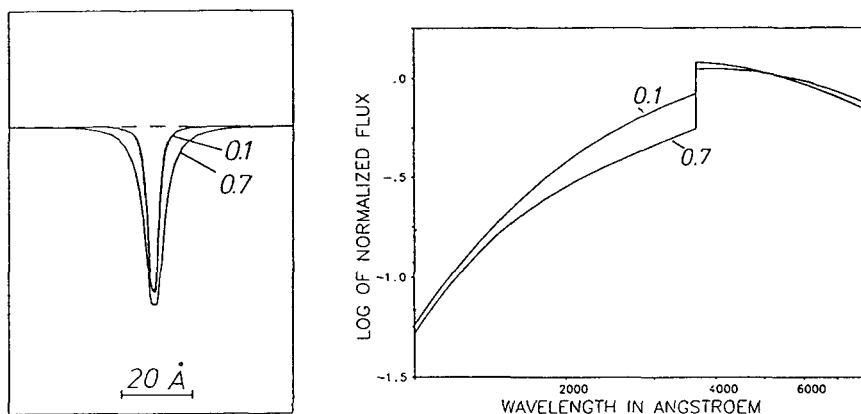


Fig. 3a: H_{γ} profiles (left) and energy distribution (right) of a typical AO Ia supergiant photospheric model with two different values of $N_{\text{He}}/N_{\text{H}}$.

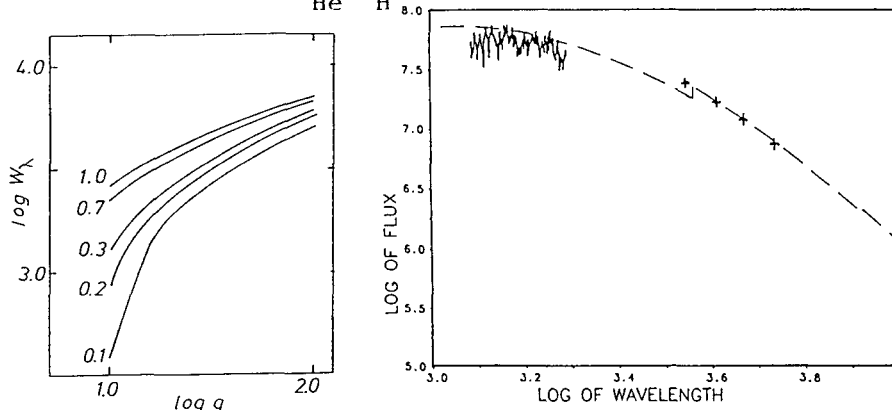
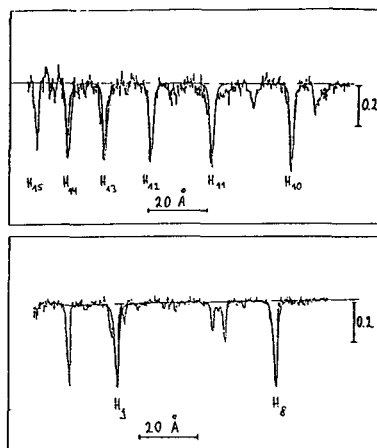


Fig. 3b (upper left): \log of H_{γ} equivalent width for models at $T_{\text{eff}} = 10^4 \text{ K}$ and different $\log g$ and $N_{\text{He}}/N_{\text{H}}$. (3a and 3b from Kudritzki, Groth, Humphreys, in prep.).

Fig. 5a (upper right): The observed energy distribution of R 71 compared with an unblanketed NLTE model of $T_{\text{eff}} = 14000 \text{ K}$, $\log g = 1.6$, $y = 0.09$.

Fig. 5b (right): Fit of the Balmer lines of R 71 with the final hydrostatic NLTE model.



An additional important effect is the "wind-blanketing" (see Abbott and Hummer, 1985). As a consequence, the spectral types show an additional dependence on the stellar mass-loss rate. For the sake of brevity, we omit a fuller discussion at this point.

2.2. O-stars in Galaxy, LMC, SMC

The application of the method of detailed photospheric NLTE analysis on O-stars has been reviewed very recently by Ku 88. We therefore summarize only the most important issues: Very massive stars with $M \geq 100 M_{\odot}$ exist not only in the Galaxy (Kudritzki, 1980, Simon et al., 1983) but also in the LMC (Gehren et al., 1986) and even in the SMC (Kudritzki et al., 1988a). For supergiants like ζ Puppis (O4 f), α Cam (O9.5 Ia) in the Galaxy or Sk 80 (O7 Iaf) in the SMC photospheric helium enrichment is very common (Kudritzki et al., 1983, Bohannan et al., 1986, Voels et al. 1988, Kudritzki et al., 1988b). This means that the effects of mixing are stronger than normally predicted by evolutionary calculations.

2.3. B-supergiants in Galaxy, LMC and SMC

As part of an extensive spectroscopic project on the formation and evolution of massive stars in parent galaxies of different metallicity, B-supergiants in Galaxy, LMC and SMC have been studied (R.P.Kudritzki, H.G. Groth, K. Butler, D. Husfeld, S. Becker, F. Eber, E. Fitzpatrick). The results obtained so far are summarized in Table 1:

Table 1a: the objects

star	spectral type	V	B-V	galaxy
Sk 21-65 ^o	B0 Ia	12.02	-0.14	LMC
Sk 41-68 ^o	B0.5Ia	12.01	-0.14	LMC
HDE 268685	B1 Ia	11.52	-0.10	LMC
Sk 213-69 ^o	B1 Ia	11.97	-0.10	LMC
HDE 269504	B2 Ia	11.95	-0.09	LMC
Sk 159	B0.5Ia	11.88	-0.13	SMC
Sk 119	B2 Ia	12.19	-0.09	SMC
ϵ Ori	B0.Ia	1.70	-0.19	GALAXY
κ Ori	B0.5Ia	2.04	-0.18	GALAXY

Table 1b: stellar parameters

	T_{eff} K	$\log g$ cgs	y	R/R_{\odot}	$\log L/L_{\odot}$	$M_{\text{ZAMS}}/M_{\odot}$	$M_{\text{grav}}/M_{\odot}$
Sk 21-65°	27000	2.70	0.35	30	5.63	27	16
Sk 41-68°	25000	2.60	0.23	32	5.55	22	15
HDE268685	22000	2.35	0.23	45	5.63	27	16
Sk213-69°	22000	2.40	0.15	48	5.68	30	21
HDE269504	20000	2.25	0.23	40	5.36	14	10
Sk 159	25000	2.55	0.35	47	5.89	47	29
Sk 119	20000	2.30	0.15	51	5.57	24	19
ϵ Ori	26000	2.75	0.20	29	5.54	22	17
κ Ori	25000	2.70	0.20	28	5.44	18	14

Note that $y = N_{\text{He}}/C (N_{\text{H}} + N_{\text{He}})$.

M_{grav} is obtained from the gravity, the radius from distance and observed dereddened magnitude (for further details see Kudritzki et al., 1987). The typical uncertainties are $\Delta T_{\text{eff}} = \pm 1000$ K, $\Delta \log g = \pm 0.1$, $\Delta y = \pm 0.07$, $\Delta R/R_{\odot} = \pm 10\%$, $\Delta \log L/L_{\odot} = \pm 0.1$, $\Delta M_{\text{grav}}/M_{\odot} = \pm 30\%$.

The most striking result is that all objects are helium enriched with a large scatter in y . This again confirms observationally that mixing must be more effective than commonly thought. (For metal abundances see Kudritzki et al., 1987).

2.4. Quantitative spectroscopy of the "subluminous" LBV R 71 at minimum

Up to now LBVs have never been the subject of detailed quantitative photospheric NLTE spectroscopy. The major reason for this is that it is hard to find appropriate "photospheric" lines that are undisturbed by the emission or absorption of the surrounding wind. However, a good candidate is R 71, which has been studied by Wolf et al. (1981) during minimum on the basis of IIaO Coudé plates and IUE spectra. Their estimates for the properties of R 71 in minimum stage were: $\log L/L_{\odot} = 5.3$, $R/R_{\odot} = 81$, $T_{\text{eff}} = 13600$ K, $v_{\infty} = 130$ km s⁻¹, $\dot{M} = 3 \times 10^{-7} M_{\odot}/\text{yr}$. With this luminosity the object is about 0.6 dex below the Humphreys-Davidson limit.

Stahl, Wolf and Zickgraf have recently secured several ESO 3.6m CASPEC CCD spectra of high resolution and high signal to noise, which extend almost up to the Balmer edge and which were taken during different minimum stages. Since the higher Balmer lines in this phase are obviously undisturbed by wind effects, these spectra make it possible to

determine the gravity of R 71 directly and thus to impose an important additional constraint on its evolutionary status. Our analysis technique was therefore applied (H.G. Groth, R.P. Kudritzki) to R 71 in the usual way:

The effective temperature is found from the dereddened ($E_{B-V} = 0.1$ to 0.15) energy distribution using photospheric NLTE $B-V$ models (Fig. 5a). We obtain $T_{\text{eff}} = 14000$ K (Note that with a blanketed LTE model we would get 13500 K). $\log g$ is determined from all the Balmer lines from H_{15} down to H_8 . Simultaneously the helium abundance is obtained from the weakest He I absorption lines. The final result (see Fig. 5b) is $\log g = 1.5$, $y = 0.30$. Thus R 71 is a further example of an evolved massive star with a helium enriched atmosphere! Placing the object in both the HR and the ($\log g$, $\log T_{\text{eff}}$)-diagram we get the same answer: R 71 is most probably an object with a ZAMS mass of about $25 M_{\odot}$ on its way back from the RGB. Its present mass of 8° to $10 M_{\odot}$ ($\log g$ 1.5 to 1.6) confirms this conclusion.

We will continue with this project and determine metal abundances in future work.

3. WINDS OF LUMINOUS BLUE STARS

3.1. Observed wind properties and the recent progress of the theory

As has been proved convincingly by Lucy and Solomon (1970) and Abbott (1979), the winds of stars more massive than $15 M_{\odot}$ are basically radiation driven (for a recent discussion see Ku 88). Castor, Abbott and Klein (1975, "CAK") were the first to formulate the theory of line driven winds in a self-consistent way. In its later version (Abbott, 1982) the theory used a realistic line list of 250000 lines of H to Zn in ionization stages I to VI. The predictions of the theory were:

$$v_{\infty} = (\alpha/(1-\alpha))^{1/2} v_{\text{esc}}$$

$$\dot{M} \sim L^{1/\alpha} (M(1-L/L_E))^{1-1/\alpha}$$

The parameter α comes out as a result of the theory and lies between 0.5 and 0.7. L_E is the Eddington luminosity. As is well known (see Ku 88), these predicted proportionalities are roughly reproduced by the observations. However, the old CAK theory fails with respect to the proportionality constants. Predicted mass-loss rates are too high by a factor of three and theoretical terminal velocities too low by a large factor. Since v_{∞} can be measured with high precision, the latter discrepancy cast enormous doubts on the theory.

However, Pauldrach et al. (1986) were able to prove that this failure was caused by the "radial streaming ap-

proximation" made by CAK. Relaxing this approximation they showed that radiation driven wind theory can reproduce the observed \dot{M} and v_∞ . In a next step, Kudritzki et al. (1987) applied the theory to low metallicity O-stars as are to be found in the SMC and LMC and reproduced the lower v_∞ observed for these objects by Garmany and Conti (1985).

The most important improvement concerns the calculation of the occupation numbers in the stellar wind plasma. For correct radiation hydrodynamics and spectral diagnostics accurate calculations for all ions driving the wind are inevitable. For a long time occupation numbers in the wind were computed in a very approximate way. Recently the first realistic calculations became available. Pauldrach (1987) adopted a cool wind ($T_w \approx T_{\text{eff}}$) and treated the full multi-level NLTE problem of all relevant elements and ions including electron collisions self-consistently with the radiation driven wind hydrodynamics. He includes 26 elements, 133 ionization stages, 4000 levels and 10000 radiative bound-bound transitions in the rate equations and the correct continuous radiation field for the bound-free rates calculated from the spherical transfer equation. Puls (1987) extended these improvements significantly by including "multiline effects". These arise from the velocity induced line overlap, which causes radiative coupling between different ions and possible multiple momentum transfer from photons to the wind plasma. The first application of this improved theory to the case of the O4f-star ζ Puppis shows excellent agreement with respect to the dynamical quantities \dot{M} and v_∞ . In addition - and this is the really important result - an enormous shift towards higher ionization stages is obtained due to the detailed NLTE treatment. Thus, it was possible to reproduce for the first time the observed high ionization features of OVI, NV, CIV etc. by cool wind models. A typical example is given in Fig. 6, which shows how perfectly the observed NV profile in the UV-spectrum of ζ Puppis can be reproduced by the self-consistent radiation driven NLTE wind model atmospheres. Note that this is not a profile fit, where \dot{M} and $v(r)$ have been adjusted as parameters. It is the result of a self-consistent calculation, that depends only on the choice of the stellar parameters $\log L/L_\odot$, T_{eff} and $\log g$.

We have now applied calculations of this type along evolutionary tracks for massive stars to investigate whether our wind models also reproduce the change of spectral morphology during stellar evolution as observed by Walborn and collaborators (Walborn and Panek, 1984a,b, 1985; Walborn and Nichols-Bohlin, 1987; Walborn et al., 1985). Fig. 7 demonstrates the extreme behaviour of the SiIV resonance lines, which exhibit a pronounced luminosity effect both in theory and observation. The physical reason for this effect, which will prove to be of enormous potential for the lumi-

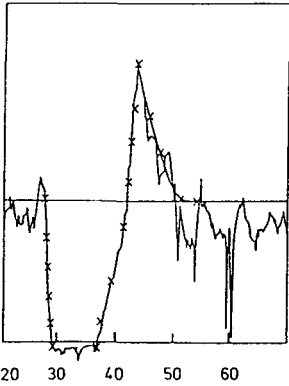


Fig. 6: The IUE high resolution profile of NV λ 1240 of ζ Puppis compared with the result from a self-consistent radiation driven wind model (crosses) (from Puls,1987).

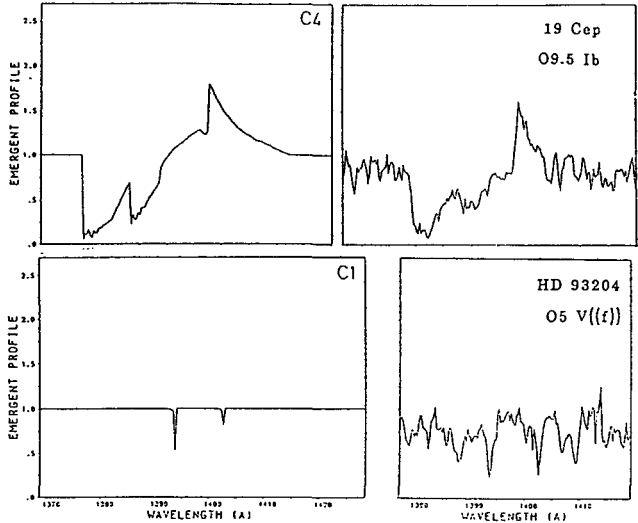


Fig. 7: The strong observed luminosity effect of SiIV as reproduced by the wind models. The observations are taken from Walborn et al. (1985). (For discussion see text).

Fig. 8a: Energy distribution of model A (fully drawn) compared with a hydrostatic model (dashed).

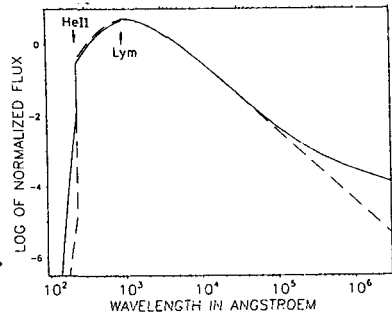
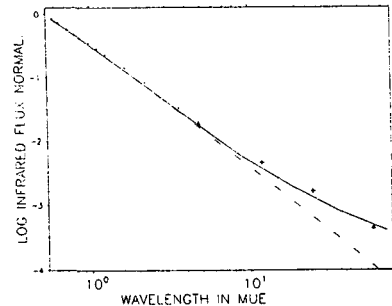


Fig. 8b: Enlarged optical and IR part of Fig. 7a compared with the observations for the O4f star ζ Puppis.



osity classification of extragalactic O-stars using HST, is that in the winds of O-stars most of the silicon is SiIV. Supergiants lie close to the Eddington limit and thus have dense winds, which lead in turn to strong recombination towards SiIV. Consequently, the SiIV wind features show up in the supergiants. The behaviour of NV, NIV, CIV can also be reproduced by the models, but this is not shown here for sake of brevity. We thus conclude that the status of the theory is very promising with respect to normal OB-stars. The question, however, is how does it work in the case of LBVs.

3.2. Wind models for LBVs

We have applied our improved radiation driven wind code to two typical LBV-stars in quiescence, R 71 and P-Cygni. We start the discussion with R 71:

As stellar parameters for R 71 in quiescence we have chosen (see section 2.4.) $\log L/L_{\odot} = 5.3$, $\log g = 1.6$, $T_{\text{eff}} = 14000$ K. The radiation driven wind hydrodynamics (including the self-consistent NLTE treatment of the radiative line force yields $\dot{M} = 3.3 \times 10^{-7} M_{\odot}/\text{yr}$ and $v_{\infty} = 225$ km/s for these parameters. This compares well with the observed values of $3 \times 10^{-7} M_{\odot}/\text{yr}$ and 127 km/s, respectively (see 2.4.). This means that R 71 in quiescence is obviously no problem for the theory.

P-Cygni, on the other hand, is far more complicated as it lies much closer to the Eddington-limit. This means that its wind properties depend strongly on the ratio $L/L_E \sim L/M$. The detailed and extensive calculations presented by Puls et al. and Pauldrach et al. (both contributed papers in these proceedings) demonstrate, however, that even in this extreme case the theory works well and reproduces \dot{M} , v_{∞} as well as the very gradual slope of $\rho(r)$ and $v(r)$, inferred from the far IR-energy distribution. Moreover, the detection of the bistability of the wind of P-Cygni due to the sudden change of optical thickness in the Lyman-continuum might provide an interesting tool for the understanding of the variability of LBV-winds!

4. UNIFIED MODEL ATMOSPHERES INCLUDING WINDS AND SPHERICAL EXTENSION

4.1. Motivation

Hydrostatic photospheric models neglect the emission of the surrounding stellar wind envelope. They are therefore unable to produce the observed wind induced strong emission features in the optical spectra of hot stars (H_{β} , HeII 4686, IR-emission) or the distortion of photospheric absorption profiles (H_{β} , HeI 5876, HeII 5412).

The normal procedure to account for these effects is to put a wind on top of a hydrostatic photosphere and then to study its influence on the spectrum. This method has crucial limitations as it makes an artificial division between photospheres and winds and introduces unnecessary free parameters which strongly influence the calculations at the borderline between the two regions (for a discussion see Ku 88 or Gabler et al., 1988). The alternative is the concept of "unified model atmospheres" introduced recently by Gabler et al., 1988. This new model atmosphere code takes \dot{M} , $v(r)$, $\rho(r)$ from the hydrodynamics of radiation driven winds (see section 2.) and calculates $T(r)$, $n_i(H)$, $n_i(He)$ by a detailed NLTE treatment using radiative equilibrium and correct spherical radiative transfer. These models need only T_{eff} , $\log g$, R_* at the inner atmospheric boundary as the natural free parameters and are in principle self-consistent. They yield the entire sub- and supersonic atmospheric structure, the stellar energy distribution and the hydrogen and helium line spectra. As has been shown by Gabler et al., the surrounding wind can have significant influence on the emergent spectrum even in cases where the wind density is not extremely strong. In the following we restrict the discussion to models for luminous O-stars.

4.2. Unified models for luminous O-stars

Four models have been calculated here with the following parameters:

model	T_{eff} (10^3 K)	$\log g$ (cgs)	$\log L/L_{\odot}$	spectral type
A	45	3.6	6.0	O4f supergiant
B	32	3.2	5.8	O9.5 giant
C	32	2.9	5.8	O9 supergiant
D	32	2.9	6.1	O9 supergiant

Note that models B and C have the same luminosity, but different gravity, whereas the opposite is true for models C and D.

For the sake of brevity we discuss only a few effects: Fig. 8 demonstrates how the energy distribution (in particular the EUV and the FIR) is affected by the wind envelope. Fig. 9 shows that for a low temperature O-giant the wind has almost no influence on the line spectrum. However, for a supergiant of the same temperature even H_{γ} is influenced by the surrounding wind and sphericity (Fig. 9). The corresponding H_{α} emission is clearly luminosity dependent (emission of model D larger than of model C). This indicates that the unified models and H_{α} line emission may provide an

independent tool for distance determinations! For future extragalactic work this will be an important path to follow. We expect the method of unified model atmospheres to become very important for all objects close to the Eddington-limit.

ACKNOWLEDGEMENTS: This work was supported by the Deutsche Forschungsgemeinschaft under grants Ku 474-11/3 and 474-13/2.

References

- Abbott, D.C.: 1979, IAU Symp. 83, p. 237
 Abbott, D.C.: 1982, *Astrophys. J.* 259, 893
 Azzopardi M.: 1981, ESO Workshop on "The Most Massive Stars", 227
 Bohannan, B., Abbott, D.C., Voels, S.A., Hummer, D.G.: 1986, *Astrophys. J.* 308, 728
 Conti, P.S., Alschuler, W.R.: 1971, *Astrophys. J.* 170, 325
 Conti, P.S., Frost, S.A.: 1977, *Astrophys. J.* 212, 728
 Dubois, P.: 1986, *Proc. IAU Symp.* 116, 415
 Fehrenbach, Ch., Duflot, M.: 1972, *Astron. Astrophys.* 21, 321
 Fitzpatrick, E.L.: 1987, *Astrophys. J.* 312, 596
 Gabler, R., Gabler, A., Kudritzki, R.P., Puls, J., Pauldrach, A.: 1988, *Astron. Astrophys.*, in press
 Garmany, C.D., Conti, P.S.: 1985, *Astron. J.* 293, 407
 Gehren, T., Husfeld, D., Kudritzki, R.P., Conti, P.S., Hummer, D.G.: 1986, *Proc. IAU Symp.* 116, p. 413
 Hummer, D.G., Abbott, D.C., Voels, S.A., Bohannan, B.: 1988, *Astrophys. J.* 328, 704
 Humphreys, R.M.: 1983, *Astrophys. J.* 265, 176
 Kudritzki, R.P.: 1973, *Astron. Astrophys.* 28, 103
 Kudritzki, R.P.: 1980, *Astron. Astrophys.* 85, 174
 Kudritzki, R.P., Simon, K.P., Hamann, W.R.: 1983, *Astron. Astrophys.* 118, 245
 Kudritzki, R.P., Pauldrach, A., Puls, J.: 1987, *Astron. Astrophys.* 173, 293
 Kudritzki, R.P., Groth, H.G., Butler, K., Husfeld, D., Becker, S., Eber, F., Fitzpatrick, E.: 1987, *Proc. ESO Workshop on "SN 1987a"*, ed. I.J. Danziger, p. 37
 Kudritzki, R.P., Groth, H.G., Husfeld, D., Hummer, D.G., Conti, P.S.: 1988b, *Astron. Astrophys.*, in prep.
 Kudritzki, R.P., Cabanne, M.L., Husfeld, D., Niemela, V.S., Groth, H.G., Puls, J., Herrero, A.: 1988a, *Astron. Astrophys.*, submitted
 Kudritzki, R.P.: 1988, "The Atmospheres of Hot Stars: Modern Theory and Observation", 18th Advanced Course, Swiss Society of Astronomy and Astrophysics, Leysin, March 1988
 Lucy, L.B., Solomon, P.: 1970, *Astrophys. J.* 159, 879

- Maeder, M., Meynet, G.: 1987, *Astron. Astrophys.* 182, 243
 Pauldrach, A., Puls, J., Kudritzki, R.P.: 1986, *Astronom. Astrophys.* 164, 86
 Pauldrach, A.: 1987, *Astron. Astrophys.* 183, 295
 Puls, J.: 1987, *Astron. Astrophys.* 184, 227
 Simon, K.P., Jonas, G., Kudritzki, R.P., Rahe, J.: 1983, *Astron. Astrophys.* 125, 34
 Voels, S.A., Bohannan, B., Abbott, D.C., Hummer, D.G.: 1988, *Astrophys. J.*, in press
 Walborn, N.R., Panek, R.J.: 1984, *Astrophys. J.* 280, L27
 Walborn, N.R., Panek, R.J.: 1984, *Astrophys. J.* 286, 718
 Walborn, N.R., Panek, R.J.: 1985, *Astrophys. J.* 291, 806
 Walborn, N.R., Nichols-Bohlin, J., Panek, R.J.: 1985, "IUE Atlas of O-Type Spectra from 1200 to 1900 Å", NASA Reference Publication 1155
 Wolf, B., Appenzeller, I., Stahl, O.: 1981, *Astron. Astrophys.* 103, 94

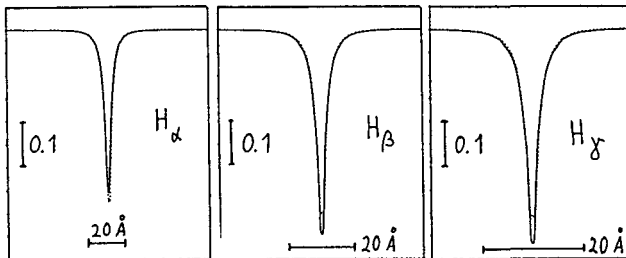


Fig. 9: The Balmer lines of model B (dots: hydrostatic, fully drawn: unified model).

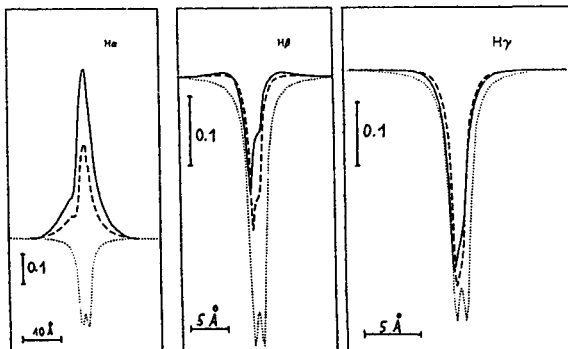


Fig. 10: The Balmer lines of model C (dashed) and model D (fully drawn) compared with the hydrostatic model (dotted).

DISCUSSION

Maeder: Your beautiful results represent an essential constraint for understanding stellar evolution. Surface helium and nitrogen enrichments in models are usually produced by a number of physical effects: convective dredge-up, mass loss, overshooting, intermediate convective zone, *etc.* These effects lead to considerable He and N enrichments for stars in some parts of the H-R diagram (*cf. Astr. & Astrophys.* 173, 287): very massive O stars, red supergiants, blue supergiants, WR stars. The main question now is: do the observations and evolutionary predictions correspond? If yes, OK; if no, this means that new mixing mechanisms have to be included to reproduce the richness of Nature. In the case of O stars, we already know that in order to account for the data we must assume that a fraction of the O stars evolve close to homogeneity. Shall we have to assume something similar for B supergiants?

Kudritzki: Well, all I can say now is that it looks like this.

Davidson: It seems to me that the most urgent goal for LBV studies now is to explain and quantify their eruptive instability; no one can safely claim to understand the upper H-R diagram until this has been done. From this point of view, the most important thing in your talk is the "bistability" that arises in your group's analysis of P Cygni. It would be good to know more about the mutual similarities and differences among the phenomenon that Andre Maeder proposed, Immo Appenzeller's bimodal ideas that he will probably discuss, and the bistability that you have found. But for now, here's an assertion that may seem cryptic but which will probably be specified better sometime later at this meeting (I will do it myself if nobody else does): If we simply take a fixed value of the radiation-force gallows Γ_{crit} defined in a particular way, and suppose that your bistability or something very much like it occurs near that value, then we can reproduce the observed Upper Limit in the H-R diagram. This is a quantitative conjecture, based on some idealized figuring.

Walborn: Janet Drew finds that when the wind temperature is derived from the model rather than adopted or similar to T_{eff} , it is significantly lower and the super-ionization is not reproduced. Do you expect your new united models to resolve this discrepancy?

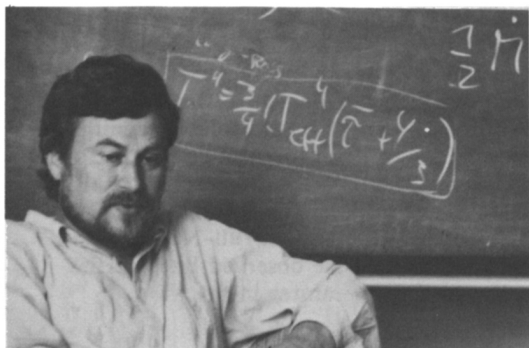
Kudritzki: Janet's calculations are in radiative equilibrium and include the important effect of cooling by metal lines. However, two crucial simplifications are still present in her calculations: an approximate treatment of optically thick continua, and ionization from excited levels. The situation with respect to radiative equilibrium is not clear until the models are improved. In our unified models, which at present treat only hydrogen and helium, the next step to be done by Rudi Gabler will be the correct inclusion of the most important metals, avoiding these simplifications. A check on the radiative equilibrium will then be possible. If radiative equilibrium is not fulfilled, as I expect for the outer wind layers, then this will be a direct proof of the importance of dissipative processes as calculated by Stan Owocki and his collaborators. The only way to investigate this is to do first the full NLTE calculations, including radiative equilibrium correctly. Our present full-NLTE wind calculations for adopted $T_{\text{wind}} \sim T_{\text{eff}}$, which nicely fit the observed line profiles, can then be used as constraints for the observed temperatures in the wind.

Cassinelli: X-rays can have a major effect on the super-ionization stage. There is evidence for a significant X-ray intensity in ζ Puppis, for instance. Given that, it is surprising to hear you say that the observed super-ionization can be explained without accounting for X-rays. Were you able to produce the strong OVI $\lambda 1040$ line seen in ζ Pup with your model?

Kudritzki: There is no doubt that the X-rays are there. Whether they affect the ionization equilibrium depends on assumptions about the layers in the wind where they originate. Pauldrach has discussed this (1987; *Astr. & Astrophys.* 183, 295), finding that if the observed X-ray flux originates from the full wind volume, then the mean X-ray ionization rate is small compared to ionization caused by optically thick radiation shortward of 228 \AA (the He II edge), which is treated correctly in our calculations. However, if we assume that the X-rays come from the outer wind layers only, *i.e.* where $v(r) \geq 0.8v_\infty$ (which is supported by observations), then they are very important for ionization in these layers. This is a nice coincidence, since Pauldrach can reproduce observable OVI only up to $0.8v_\infty$ in the case of ζ Puppis. This means that we have an indication that the correct NLTE treatment is sufficient in the whole wind region, but that in the outermost layers X-ray Auger ionization has to be included in the rate equations. This can be done easily in our code, provided we have the local mean X-ray intensity in the wind. To get this in a more self-consistent way, one has to follow and to extend the impressive work by Owocki/Castor/Rybicki, who by elaborate time-dependent hydro-calculations investigate wind instabilities and the corresponding evolution of dissipative shocks. We will follow this line.

Humphreys: In your talk you mentioned an initial mass around $25 M_\odot$ for R 71. What is its current "spectroscopic" mass? You also mentioned $23 M_\odot$ from your spectroscopic analysis of P Cygni. These masses are not inconsistent with evolutionary models, especially when we consider that LBV's are in a rapid-mass-loss phase.

Kudritzki: I agree, $23 M_\odot$ for P Cyg fits perfectly with Maeder/Meynet at $\log L/L_\odot \sim 5.8$ and $T_{\text{eff}} \sim 19000 \text{ K}$. I did the same exercise with R 71 and it agrees also, $\sim 10 M_\odot$ indicated by the $\log g$, $\log T_{\text{eff}}$ diagram. So we have no disagreement for these stars but we have the "normal" B0 Ia, B1 Ia supergiants; all the stars analyzed by us so far show the enrichment, which disagrees with our expectation that only those returning from the red giant branch should be enriched and not those on their way to the RGB.



Rolf Kudritzki
(reflecting on boundary conditions)